Uniqueness of Multiangular Measurements—Part I: An Indicator of Subpixel Surface Heterogeneity From MISR

Bernard Pinty, Jean-Luc Widlowski, Nadine Gobron, *Member, IEEE*, Michel M. Verstraete, *Member, IEEE*, and David J. Diner, *Associate Member, IEEE*

***Abstract*—The recent availability of quasi-simultaneous multispectral and multidirectional measurements from space, as provided by the Multi-angle Imaging SpectroRadiometer (MISR) on board the Terra platform, offers new and unique opportunities to document the anisotropy of land surfaces at critical solar wavelengths. This paper presents simple physical principles supporting the interpretation of the anisotropy of spectral radiances exiting terrestrial surfaces in terms of a signature of surface heterogeneity. The shape of the anisotropy function is represented with two model parameter values which may be mapped and interpreted in their own right. The value of one of these parameters also permits identifying geophysical conditions where the surface heterogeneity becomes significant and where three-dimensional (3-D) radiation transfer effects have to be explicitly accounted for. This paper documents these findings on the basis of results from a number of 3-D radiation transfer model simulations. The latter are used to perform an extensive sensitivity study which includes issues related to the scale of investigation. A preliminary validation of these results, conducted with a dataset collected by the AirMISR instrument over the Konza prairie, is also discussed.**

***Index Terms*—k parameter, MISR, RPV model, surface heterogeneity.**

I. Introduction

THE RECENT availability of quasi-simultaneous multispectral and multiangular measurements from the Along-Track Scanning Radiometer-2 (ATSR-2), the Polarization and Directionality of the Earth's Reflectances (POLDER) and the Multi-angle Imaging SpectroRadiometer (MISR), brings new and unique opportunities to develop and apply operational algorithms that capitalize on the understanding of radiation transfer processes within the atmosphere and vegetation layers, as well as at their interfaces (see, for instance, [1], for a series of examples). The primary benefits from multiangular measurements lie in an improved accuracy and reliability of the derived products thanks to the addition of appropriate constraints for identifying the solutions to a series of inverse radiation transfer problems. Although this aspect constitutes, *a priori*, a definite conceptual advantage over algorithms that can be applied on data gathered by single angle sensors, accuracy improvements might not always be systematically required for all geophysical applications. The main issue that will be addressed here is to establish whether and to what extent the acquisition of multiangular data from space permits the assessement of new and unique information on the status of terrestrial surfaces.

This and a companion paper demonstrate that such unique information can in fact be obtained by coupling new approaches with more traditional spectral analyses. This paper describes the simple physical principles supporting the interpretation of the measured anisotropy of spectral radiances exiting from terrestrial surfaces in terms of a signature of surface heterogeneity at the subpixel scale. The angular distribution of surface leaving radiances exhibits a degree of anisotropy which can be characterized through the parameter values entering the angular function of the model developed by Rahman *et al.* (the so-called RPV model [2]). The degree of anisotropy of these surface radiance fields can therefore be assessed, mapped, and interpreted in its own right. The conceptual developments presented in this paper also demonstrate that one of these parameters has the potential to expose significant surface heterogeneity at the subpixel scale. Beyond information about the heterogeneity of the surface, the value of this parameter also permits identifying geophysical conditions where the three-dimensional (3-D) radiation transfer effects have to be explicitly accounted for. In a companion paper ([3], hereafter referred to as Part II), we show that the angular domain of measurement can be combined with the spectral domain in order to deliver jointly information about the photosynthetic activity and structure of vegetation: a spectral axis yields a quantitative estimate optimally related to the FAPAR through the combined use of the blue, red, and near-infrared spectral bands; a structural axis, independent from the first one, corresponds to the surface heterogeneity parameter optimally retrieved from an analysis of the angular measurements made in the red band only. The approach presented in these two papers has been prototyped for the AirMISR and MISR instruments, providing a good compromise between the desired angular and spectral sampling of the radiance field and the spatial resolution of data acquisition.

II. Interpretation of the Anisotropy of Surface Leaving Radiance Fields

A. Surface Anisotropy as a Unique Feature

All surfaces, natural or man-made, show some degree of spectral anisotropy when illuminated by a point source of light in the solar domain, i.e., the bidirectional reflectance factors (BRFs) of these media vary with both the illumination and observation

Manuscript received August 24, 2001; revised March 26, 2002.

B. Pinty, J.-L. Widlowski, N. Gobron, and M. M. Verstraete are with the Institute for Environment and Sustainability, European Commission Joint Research Centre, I-21020 Ispra (VA), Italy (e-mail: bernard.pinty@jrc.it).

D. J. Diner is with the Jet Propulsion Laboratory, California Institute of Technology, Pasadena, CA 91109 USA.

Publisher Item Identifier 10.1109/TGRS.2002.801148.

angular locations [4]. Since this surface anisotropy depends on the structure and optical properties of the observed medium, it constitutes an angular signature of the target. To the extent that this signature results from the interaction of the radiation field with the medium, a proper understanding of the relevant processes may lead to the characterization of the medium on the basis of remote sensing data. These radiative processes can be modeled and understood using radiation transfer theory and implementing the adaptation necessary to account for specific effects such as specularity and hot spot scattering enhancements (see [5]). Depending on the application, surface anisotropy can be perceived either as a source of noise, e.g., when developing vegetation indices, or alternatively, as a source of information in addition to the spectral dimension, since the anisotropy exhibited by surface BRF fields is fully controlled by radiation transfer processes. In the first case, the surface anisotropy effects have to be eliminated to produce information not contaminated by the observation and illumination conditions. In the second case, the anisotropy is exploited with adequate radiation transfer tools to provide better constraints when solving the inverse remote sensing problems. This second alternative allows more parameters to be assessed, and, therefore enhances the capability of deriving accurate and reliable documentation of geophysical systems from measurements gathered in space (see, for instance, [6]).

Surface anisotropy patterns can adequately be represented by suitable parametric models. These models do not need to be based on or rigorously follow from basic physical principles to the extent that they must only be able to represent the anisotropy effects from a large variety of media in the simplest possible manner, that is with a minimum number of input parameters [7]. The recent developements of multiangle sensors has promoted the refinement of such parametric models [8] and two broad families have emerged: the linear-kernel driven models [9] and the RPV model [2]. The former assumes that the spectral BRF fields can be described as a sum of three contributions; the latter, which has a long historical development dating back to early investigations of the scattering properties of celestial bodies, proposes a representation of the same fields on the basis of three parameters entering a product of angular functions. Through its mathematical formulation, the RPV model splits a BRF field into its amplitude component and the associated angular field describing the anisotropic behavior of the surfaces under investigation when illuminated by the sun, that is

$$\rho_{sfc}(z_0, \Omega_0 \rightarrow \Omega; \rho_0, \rho_c, \Theta, k) = \rho_0 \check{\rho}_{sfc}(z_0, \Omega_0 \rightarrow \Omega; \rho_c, \Theta, k) \quad (1)$$

where Ω_0 and Ω represent the direction of incoming and outgoing radiation, respectively, and where ρ_0 and $\check{\rho}_{sfc}(z_0, \Omega_0 \rightarrow \Omega; \rho_c, \Theta, k)$ describe the amplitude and the angular variations of the surface BRF, respectively.

This latter quantity is expressed by

$$\check{\rho}_{sfc}(z_0, \Omega_0 \rightarrow \Omega; \rho_c, \Theta, k) = M_I(\theta_0, \theta; k) F_{HG}(g; \Theta) H(\rho_c; G) \quad (2)$$

where

$$M_I(\theta_0, \theta; k) = \frac{\cos^{k-1}\theta_0 \cos^{k-1}\theta}{(\cos\theta_0 + \cos\theta)^{1-k}} \quad (3)$$

$$F_{HG}(g; \Theta) = \frac{1-\Theta^2}{[1+2\Theta\cos g + \Theta^2]^{3/2}} \quad (4)$$

$$H(\rho_c; G) = 1 + \frac{1-\rho_c}{1+G} \quad (5)$$

$$\cos g = \cos\theta\cos\theta_0 + \sin\theta\sin\theta_0\cos\phi \quad (6)$$

$$G = \left[\tan^2\theta_0 + \tan^2\theta - 2\tan\theta_0\tan\theta\cos\phi\right]^{1/2} \quad (7)$$

where ρ_c is the hot spot parameter, and where θ and θ_0 are the observation and illumination zenith angles, respectively. The relative azimuth angle ϕ is zero when the source of illumination is behind the sensor.

Engelsen *et al.* [10] report in detail on the performance and limits of applicability of this parametric model. The angular function $M_I(\theta_0, \theta; k)$, i.e., the so-called modified Minnaert's function [11], permits the mathematical representation of the overall shape of the angular field through the parameter k. Specifically, k is close to 1.0 for a quasi-Lambertian surface (very limited angular variations in the spectral BRF field), k is lower than 1.0 when a bowl-shape pattern dominates (the spectral BRF values increase with the view zenith angle) and, conversely, k is greater than 1.0 when a bell-shape pattern is observed (the spectral BRF values decrease with the view zenith angle). The other angular functions controlling (2) are adding more complexity/flexibility to the anisotropy classes described above; they allow the accounting for asymmetrical shapes around the local normal to the sampled area, due to the possible imbalance between the backward and forward scattering regions, as well the backscattering enhancement due to the hot spot effect. $F_{HG}(g; \Theta)$ is based on the Henyey–Greenstein function [12], and the parameter Θ establishes the degree of forward or backward scattering, depending on its sign.

A recent paper by Pinty *et al.* [13] revealed that maps of the parameter k derived from an analysis of Meteosat data exhibit spatially consistent fields and features corresponding to known gradients in surface types which may or may not be represented by variations in the amplitude component of the BRF fields. It strongly suggests that the parameter k can be used as one additional and possibly independent axis of information to better identify and separate various surface types than is feasible on the sole basis of spectral measurements. This preliminary statement does not constitute, in itself, a new finding, since, for instance, the analysis of low resolution Nimbus 7 data acquired during the Earth Radiation Budget experiment already showed that different anisotropic factor values can be assigned to different cloud and broad surface types (see, for instance, [14]). One can thus easily foresee that, thanks to their capability to measure quasi-instantaneously the angular radiance fields emerging at the top of the atmosphere, multiangle instruments such as POLDER, ATSR, and MISR should improve the identification of surface types through the unique assessment of their individual surface anisotropy. For instance, maps of the ρ_0 and k parameters obtained by inversion of the RPV model at various wavelengths can be ingested by classification techniques to

produce revised land cover maps and better detect changes occurring at the surface. We may anticipate that such exercises will soon become quite frequent due to the operational availability of such surface anisotropy information [15]. It is thus important to understand how the anisotropic signature of geophysical media can be interpreted and, in particular, what practical information could be derived from simple parameterizations such as the one used here.

B. Anisotropy Pattern as an Indicator of Surface Heterogeneity

The parameter k of the RPV model plays a fundamental role in representing the anisotropy of the surface.

- $k < 1.0$ corresponds to a bowl-shape anisotropy pattern where BRF values close to nadir are lower than for larger exiting angles.
- $k = 1.0$ corresponds to a Lambertian surface, an idealized case rarely found in practice.
- $k > 1.0$ corresponds to a bell-shape anisotropy pattern where BRF values measured at large exiting angles are lower than those measured at angles close to nadir.

The vast majority of terrestrial surfaces, whose anisotropy patterns have been investigated using laboratory, field, or airborne measurements, exhibit a bowl-shape anisotropy pattern. Models describing the scattering of light by homogeneous plane-parallel turbid geophysical media also typically generate this type of anisotropy pattern. Indeed, under such conditions, radiative transfer theory and, in particular, the multiple scattering component, predicts an increase of the BRF values together with the exiting zenith angle. This situation is also generally observed for closed (large values of the leaf area index) homogeneous plant canopies, bare soils, and other planetary surfaces as well.

Observations of bell-shape anisotropy patterns have been occasionally reported in the literature (see, for instance, [16] and [17]). It is thus interesting to investigate under which conditions this type of anisotropy occurs. A class of geophysical systems that exhibit a higher reflectance when observed from above than at large zenith angles can easily be conceived of: consider, for example, at red wavelengths, a sparse coniferous forest over a snow-covered field, or sparse bushes over a bright sandy desert. In such cases, the high background reflectance dominates at small observation zenith angles, while the absorbing properties of the dark objects control the reflectance of the entire scene at large angles. These BRF fields should therefore exhibit a bell-shape pattern corresponding to k values greater than 1.0 when analyzed with the RPV model.

A few critical remarks are in order at this point.

- If the density of the dark vertical structures increases sufficiently, the reflectance field of the system will tend toward that of a fully covered but "homogeneous system" of such structures, and the anisotropy pattern will be bowl-shaped.
- If the density of the dark vertical structures decreases to low values, the bright underlying surface will control the anisotropy of the scene at all angles, and the reflectance will also tend to correspond to a bowl-shape.
- Only rather heterogeneous geophysical systems composed of relatively sparse dark vertical structures over a bright background can lead to anisotropy patterns characterized by a bell-shape.

In fact, it is the main thesis of this paper that a bell-shape anisotropy pattern over vegetated surfaces characterized by $k > 1.0$ likely identifies heterogeneous systems composed of sparse dark vertical structures over a relatively brighter surface at the subpixel spatial resolution. This numerical condition can thus be considered as an indicator of surface anisotropy in the sense described above. This, however, does not imply that all forms of heterogeneity will result in a bell-shaped anisotropy pattern. Incidentally, whenever heterogeneity is detected in the sense of this protocol $(k > 1.0)$, the principle of reciprocity will likely not be valid. The implications of this fact will be discussed later.

The essence of our interpretation lies in the presence of vertically distributed absorbing material (e.g., vegetation at the red wavelength because of the presence of strongly absorbing chlorophyll bands) overlying a brighter (more reflecting or less absorbing) interface or lower boundary condition (e.g., the vast majority of soils at the red wavelength). Actual situations are of course very complex: the reflectance of each pixel of a heterogeneous system viewed from the nadir depends on competing factors such as the intrinsic optical properties of the scene elements but also the presence of shadows induced by the vertical stands. However, it should be noted that even one-dimensional (1-D) models, simulating the radiation transfer regime in vegetation canopies, can generate bell-shaped anisotropy patterns, if the former explicitly account for the finite-size of the elementary scatterers, i.e., the leaves. This may occur when the model input variables are set up to represent, for instance, open (low values of the leaf area index) canopies, especially under conditions where the leaf angle distribution favors an erectophile leaf orientation: the heterogeneity of the canopy system is, indeed, inherent to the presence of finite-size oriented leaves. The same conclusion applies for bare soils exhibiting significant roughness that will create well-marked shadows.

For all practical purposes and considering typical values for the vegetation architectural attributes, a medium spatial resolution sensor (a few tens to hundreds of meters) has the potential to expose subpixel scale surface heterogeneity controlled by the presence of clumped vegetation as is the case for open forest and woodland ecosystems. In principle, under ideal situations, the potential to detect structural heterogeneity is independent of the spatial scale corresponding to the pixel size. This structural heterogeneity may, however, be more difficult to detect using a low spatial resolution sensor, since it is likely that larger pixels incorporate a variety of surface types and the radiative angular effects due to the structurally heterogeneous fraction are smeared by the presence of a mixture of various surface types.

Fig. 1 illustrates the evolution from a quasi-1-D, i.e., uniformly distributed leaves are the major scattering elements, to a complex 3-D radiative transfer regime due to the significant impact of horizontally distributed vertical structures occurring in the latter case, i.e., the vegetation is structurally organized at a higher level than the leaf level. The top panels provide a visualization of a simulated quasi-1-D scene (top left) together with the corresponding BRF values generated in the cross plane (top right), i.e., the plane perpendicular to the principal

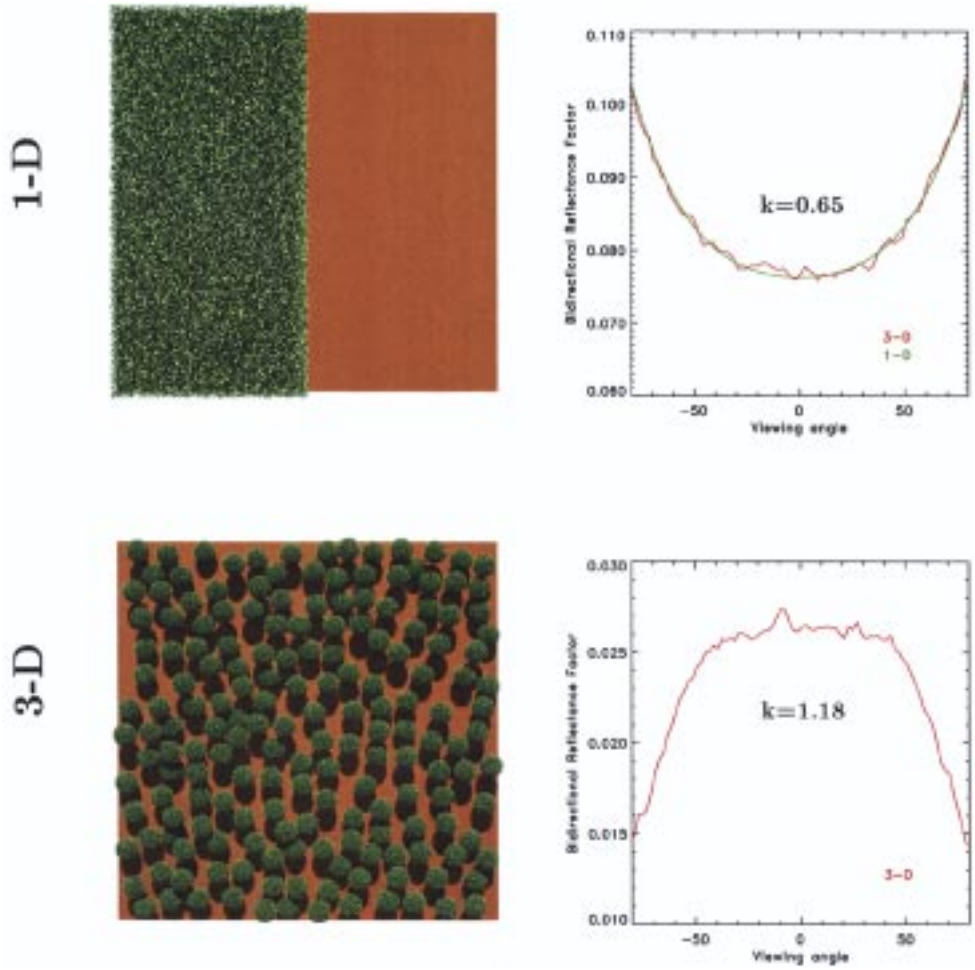

Fig. 1. Typical angular signatures of the BRF field in the red spectral region emerging from quasi-1-D (top panels) and 3-D (bottom panel) vegetation scenes. Both scenes are composed of identical leaf and soil material exhibiting exactly the same radiometric properties in the two experiments. The scene leaf area index is equal to four in both cases. The left panels provide an artistic view of the scenes and the right panels show the corresponding BRF field derived from model calculations in the cross plane. In the right panels, the red (green) lines correspond to the BRF generated by the 3-D (1-D) model.

plane. These BRF values are calculated using a Monte Carlo ray-tracing model developed by [18] (red line) and the model from [19] applicable for 1-D horizontally infinite canopy scenes (green line). In the latter case, the total BRF field emerging from the scene is approximated with a linear mixing of the respective contributions due to the vegetated and bare soil domains composing the scene, i.e., it follows the Independent Pixel Approximation (IPA) scheme promoted by [20] in the case of cloud scenarios. In this first scenario, the leaves are concentrated and grouped in one part of the scene and, thus, the heterogeneous 3-D effects between the canopy and the bare soil are limited to the single straight boundary separating these two media in the horizontal plane. Therefore, since both models by [18] and [19] have already been shown to produce very accurate and reliable solutions in the simulation of the BRF fields in 1-D cases, respectively [21], they generate essentially similar and thus undiscernable averaged BRF fields.

By contrast, the bottom panels of Fig. 1 show a geophysical situation where the 3-D effects are enhanced due to the regrouping of the leaves into clumps scattered throughout the scene. In this second, architecturally more complex scenario, the BRF values are realistically simulated using the Monte Carlo ray-tracing model [21].

It is noteworthy that the only difference between the two scenarios lies in the spatial distribution of the leaves in the scene, i.e., the leaf area index (LAI), the spectral, and geometrical properties of the leaves and the soil are all set at the same values in both experiments. This structural difference, discernable through the occurrence of vegetation clumps, is, however, at the origin of a significant change in the resulting BRF values and shapes. Indeed, the BRF anisotropy patterns evolve from a bowl-shape in the quasi-1-D scenario to a bell-shape when 3-D effects become more significant. As a matter of fact, the inversion of the RPV model (following the simple procedure described in [22] and summarized in the Appendix of Part II) against these two simulated BRF data sets result in mean values for the parameter k equal to 0.65 (top panel) and 1.18 (bottom panel), respectively.

Results from these simulation scenarios reinforce the suggestion that the k parameter of the RPV model can be further interpreted as a heterogeneity indicator controlled by the occurrence of vertical structures. Although a surface application is considered here for the sake of explanation, a similar reasoning can be applied for different geophysical systems showing the required elements and for which the BRF field can be sensed at the appropriate wavelength. According to our conceptual ap-

proach, it should be enough for the parameter k to exceed the threshold value 1.0 to indicate reliably the occurrence of significant surface heterogeneity at the subpixel scale. In practice, this threshold becomes a transition zone around the value 1.0 because the inversion procedure often delivers a range of values for the parameter k, i.e., there is often no unique solution, and also because of errors on the retrieved values themselves due to uncertainties on the surface BRF fields. This particular issue is addressed and documented in Section II-C.

C. Potential and Limitation in the Exposure of Surface Heterogeneity

Considering further the generic case of an open vegetation layer sensed at the red wavelength it can, therefore, be logically expected that

- too sparse a vegetation system may not lead systematically to $k > 1.0$ conditions: there might not be enough vegetation to compensate, at large view angles, for the BRF increase due to the illuminated soil in between the vegetation elements. This system could, in fact, be almost indistinguishable from a plane-parallel system, in the sense that the BRF fields estimated with the IPA are extremely close to those obtained with the full 3-D model, except in the vicinity of the hot spot angular region;
- too dense (closed) a vegetation system will also hardly translate into $k > 1.0$ estimation: the heterogeneity might not be significant enough to create a detectable BRF increase signature at angles close to nadir, i.e., the latter might always be masked by the shadowing effects. As in the previous case, we may in fact deal with a system that could satisfy the usual plane-parallel assumption from a radiation transfer point of view.

In order to assess our expectations, we replicated the numerical experiment presented in Fig. 1 for 11 different scenarios, simulating the effects of a progressive increase in LAI and, thus of the fractional vegetation cover of the scene. A sample of the corresponding quasi-1-D and full 3-D scenes can be visualized in Fig. 2, and detailed information regarding the structural and radiative properties of the scenes are provided in Tables I–III. As already mentioned when presenting results from Fig. 1, the only changes occuring in the characteristics of the scenes between the quasi-1-D and the 3-D concern the spatial distribution of the leaves into spherical clumps. As a matter of fact, for a given scene, quantities such as LAI are conserved independently from the strategy adopted to spatially distribute the scattering elements. The geometrical projection of the spheres onto the ground can be seen in Fig. 2 especially for scenes implementing low LAI conditions[1]. In the following, and as suggested from results shown in Fig. 1, the BRF fields emerging from the quasi-1-D scenes were approximated using the model by [19] together with an IPA scheme. In the case of the 3-D scenes, the model from [18] was applied to simulate the BRF fields at the resolution of the scene.

The inversion of the RPV model was performed against the simulated BRF fields for these two ensembles of 11 scenes, each

[1]Architectural parameters imposed in Table III may generate full circular shadows onto the ground, since the spheres are allowed to "float" between predefined lower and upper levels.

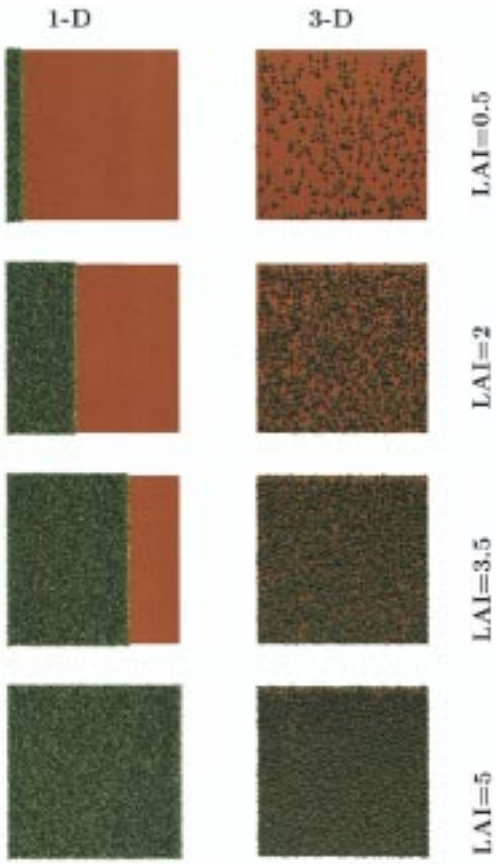

Fig. 2. Visualization of a sample of the series of 11 scenes idealizing the quasi-1-D (left panels) and corresponding 3-D (right panels) scenes for various values of the leaf area index.

TABLE I
VARIABLES DEFINING THE LEAF AND SOIL SPECTRAL PROPERTIES

Variable identification	Values
Leaf reflectance †	0.0546
Leaf transmittance †	0.0149
Soil Lambertian albedo	0.1270

† Using a bi-Lambertian scattering law.

TABLE II
VARIABLES DEFINING THE STRUCTURE OF THE QUASI–1-D SCENES

Variable identification	Values
Height of the canopy	15 m
Equivalent leaf diameter	0.05 m
Leaf Angle Distribution	uniform
Scene Leaf Area Index (LAI)	0.05 and from 0.50 to 5.0 in steps of 0.50 m^2/m^2
Ground fraction covered by vegetation	0.01 and from 0.10 to 1.0 in steps of 0.1

TABLE III
VARIABLES DEFINING THE STRUCTURE OF THE 3-D SCENES

Variable identification	Values
Sphere diameter	5 m
Leaf Angle Distribution	uniform
Leaf Area Index of the spheres	5 m^2/m^2
Maximum height of the canopy	16 m
Minimum height of the canopy	4 m
Scene Leaf Area Index (LAI)	same as in Table II
Ground fraction covered by vegetation	0.01, 0.09, 0.17, 0.26, 0.34, 0.41, 0.49, 0.55, 0.61, 0.66, 0.71

scene being considered separately, and the three RPV model parameters were thus optimally retrieved with their corresponding uncertainty levels. Fig. 3 (top panel) shows the mean and the associated uncertainty values obtained for the parameter k in the case of both the quasi-1-D and 3-D scenes, when the direct illumination source is located at 30° zenith angle, as a function of the LAI of each scene such as illustrated in Fig. 2. As could be expected from the preceeding qualitative reasoning, this figure demonstrates the potential to document the structural heterogeneity of the scenes through the value of the parameter k. Indeed, while this parameter takes on values close to unity for both low and high vegetation cover conditions, its values clearly rise to much larger values at intermediate situations, where the heterogeneous effects are maximized by the clumping of leaves into spheres. By contrast, the values of the parameter k remain within the same range, typically from 0.9 to 1.05, independent of the vegetation cover, for the associated quasi-1-D scenes. Variations in the spectral and architectural properties of the vegetation attributes may yield different relationships between the leaf area index of the scenes and the values of the parameter k. The same result holds for different sun angle conditions as mentioned already in Section II-B. Nevertheless, the presence of significant heterogeneity (in the 3-D scenarios) will translate into larger k values than would be retrieved from limited heterogeneity (idealized by the quasi-1-D scenarios) situations. Fig. 3 shows that such structural heterogeneity can be exposed over a broad range of realistic leaf area index conditions.

Other sets of analogous figures can be drawn using other quantitative variables to represent the type of scene as there is always some degree of correlation between the type of scene and, for instance, the LAI of the scene, the fractional cover, as well as the fraction of radiation absorbed by the vegetation. For instance, the bottom panel of Fig. 3 displays the variation of the k parameter for the quasi-1-D and associated 3-D scenes, as a function of the fraction of radiation absorbed by the vegetation elements composing the scenes. The use of the latter variable to define the x-axis permits us to represent the dependency of the value of the parameter k with respect to a physical quantity characterizing the vegetation. This approach is exploited in the accompanying paper.

These results, obtained from a number of accurate model simulations and based on simple physical reasoning, demonstrate

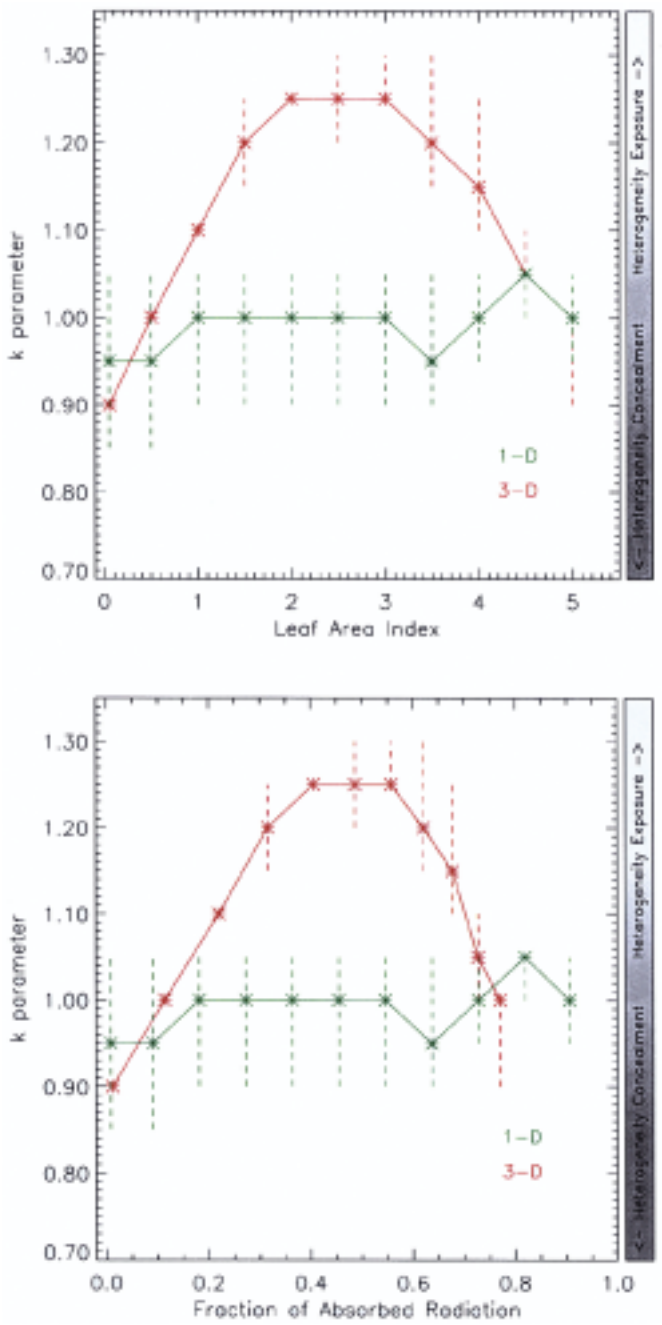

the potential for extracting unique information about structural heterogeneity of the terrestrial surfaces when sensed simultaneously at various viewing geometries and at the appropriate wavelength and spatial resolution. As explained at the beginning of Section II-B, the wavelength should be chosen so as to maximize the reflectance/absorption contrast between the vertically clumped elements and the background while the viewing geometries must permit a reliable inversion of the RPV model for the retrieval of the parameter k. Based on these considera-

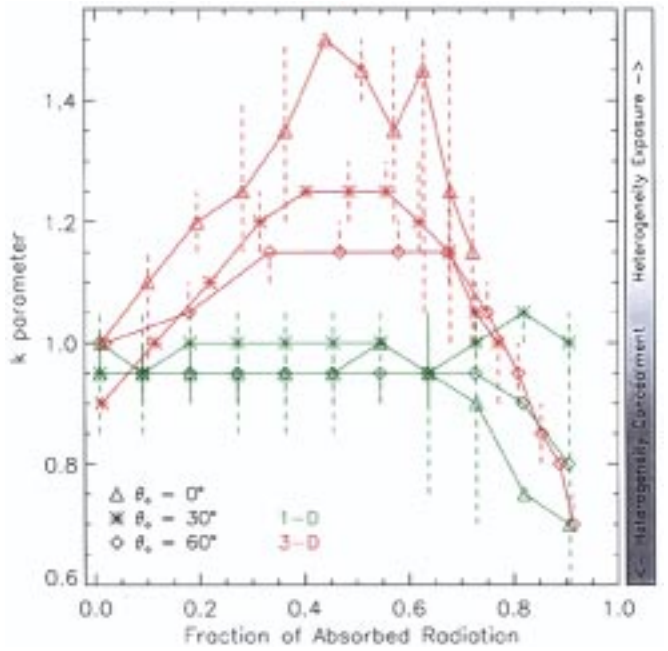

Fig. 4. Variations of the k parameter values as a function of the fraction of absorbed radiation for sun zenith angle equal to 0° (triangles), 30° (stars), and 60° (diamonds), respectively. Results obtained for the quasi-1-D and the corresponding 3-D scenes are identified with green and red colors, respectively. The vertical bars indicate the range of possible values for the k parameter that can provide an acceptable fit to the modeled BRF in each case.

tions, there is an ensemble of spectral, structural, illumination, and spatial scale aspects that will reveal heterogeneous scenes at a given sensor spatial resolution. These aspects are investigated in a quantitative manner in Sections III–V describing results obtained when performing a sensitivity analysis of the variations of the parameter k value with respect to changes in the brightness of the background, solar zenith angle, and spatial scale of investigation.

III. Sun Angle and Background Brightness Effects

Following the qualitative reasoning proposed in Section II, one can thus anticipate that the larger the spectral contrast between the soil and the vegetation (to increase the angular BRF variations between close to nadir and large view angles), and the smaller the sun zenith angle (to limit the darkening effects of shadows) the more favorable the conditions leading to the observation of k values significantly greater than 1.0.

The combined effects of changing background reflectance and illumination geometry on the retrieved values of k (or, equivalently, on the bowl or bell shape of the anisotropy) are illustrated in Figs. 4 and 5 for various types of scenes. Specifically, Fig. 4 exhibits the results obtained by replicating the simulations achieved in Section II (see Fig. 2 for quasi-1-D and 3-D scenes, respectively) for sun zenith angle values successively equal to 0°, 30°, and 60°. Results shown in Fig. 4 indicate that, as expected, the values of the parameter k decrease with an increase of the sun zenith angle: the reflectance of the background soil between the vegetation clumps becomes dominated by shadows and cannot deliver large BRF values even for viewing conditions close to nadir. This figure

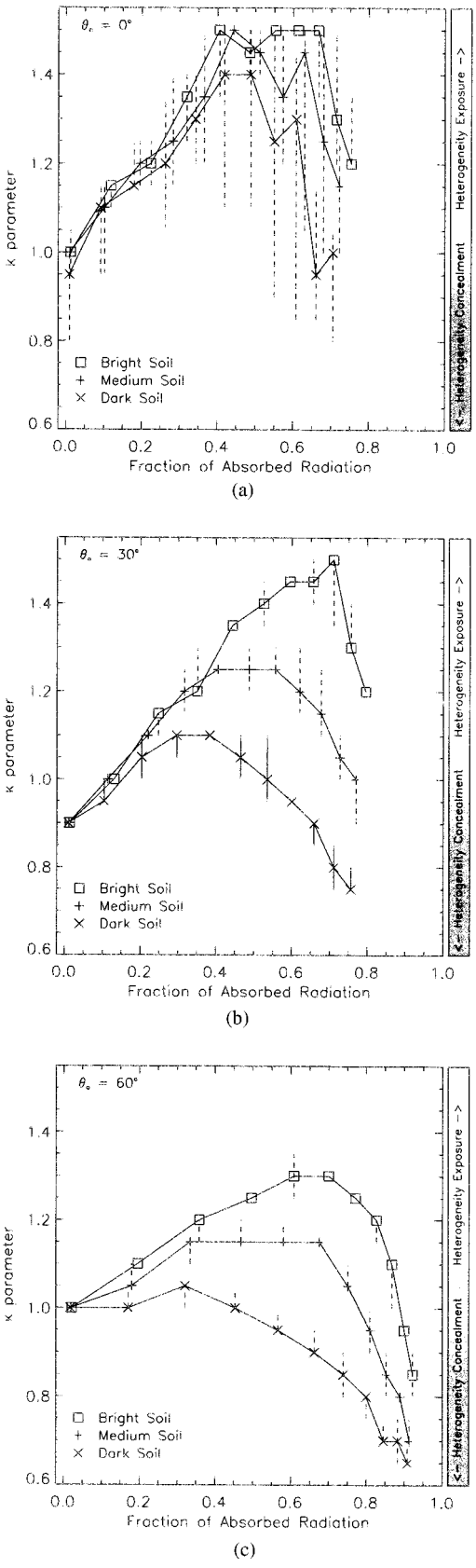

Fig. 5. Variations of the k parameter values as a function of the fraction of absorbed radiation in the case of a bright (square symbol), medium (plus symbol) and dark (cross symbol) soil albedo, respectively. Panels (a), (b), and (c) show results obtained for illumination zenith angle equal to 0°, 30°, and 60°, respectively. The vertical bars indicate the range of possible values for the k parameter which can provide an acceptable fit to the modeled BRF in each case.

shows that when the illumination angle becomes as high as 60°, the projected clump shadows are significant enough to damp the large values of the k parameter that would normally be associated with heterogeneous structures, for the spectral and architectural conditions prescribed in these simulations. By contrast, the quasi-1-D scenes are characterized by values which are always close to the 1.0 critical threshold, and under these conditions, the scene heterogeneity remains concealed.

In the same vein, the three panels in Fig. 5 display the variations in the values of parameter k estimated for three different sun zenith angles, namely 0°, 30°, and 60°, and three typical Lambert soil albedo values, namely 0.055 (dark), 0.127 (medium), and 0.242 (bright) (see [23]). It can be seen that, independent from the sun zenith angle, the brighter the soils, the larger the k parameter values, i.e., the easier it is to identify the presence of strongly heterogeneous surfaces. The observed trends followed by the k parameter values due to changes in sun zenith angle support the findings already discussed on the basis of Fig. 4. It is noticeable that, for sun zenith angles larger than 30°, a dark soil condition does not allow the anisotropy to exhibit a bell-shaped pattern, even though heterogeneity is present. However, medium or darker soil conditions are sufficient for the faint bell-shaped anisotropy to betray the existing heterogeneity with low sun conditions (see bottom panel). These simulated experiments are conducted using various soil brightness conditions for the purpose of illustrating the sensitivity of the parameter k with respect to changes in the spectral contrast between the vertical structures and the background. However, any geophysical situation exhibiting such spectral contrast would yield analogous results, independently from the intrinsic nature of both the background and the vertical elements, e.g., a snow blanket underneath a coniferous forest.

Although these results are based on a particular architecture for the specification of the 3-D heterogeneous scenes, i.e., a random distribution of vegetated clumps in the horizontal space, realistic soil, and vegetation characteristics have been used; there is, therefore, a genuine potential to actually detect in a simple manner, on the basis of the k parameter value, the occurrence of a class of heterogeneous targets, specifically those made up of dark vertically oriented architecture over a bright background. Since such spectral contrasts often occur in nature, these findings open new opportunities to characterize the heterogeneity of terrestrial ecosystems at the subpixel level, for a range of spatial scales.

IV. Application

The potential to detect structural signatures from BRF measurements hinges on the spatial scale of investigation due to the mixture of structurally heterogeneous and homogeneous surface types. It is, indeed, likely that, at lower spatial resolutions, an increasingly small fraction of the sampled scene would, on average, be displaying the characteristics of heterogeneity, i.e., greater likelihood that scenes are mixtures between heterogeneous and homogeneous surfaces, with the homogeneous fraction dominating. Accordingly, for a given terrestrial system, the retrieved value of the k parameter will strongly depend on the spatial resolution of the sensor, and the higher the spatial resolution, the more opportunities exist to expose radiatively heterogeneous systems at the subpixel resolution.

The AirMISR instrument permit accessing an intermediary spatial resolution (the nominal spatial resolution on the ground of the map-projected product is 27.5 m) which could be large enough to demonstrate the desired mechanism in the field and small enough for this mechanism to be supported from simple ground investigation. This instrument, extensively described in [24], was flown by the NASA ER-2 aircraft at an altitude close to 20 km, under almost cloud-free conditions, over the Konza prairie site in Kansas on July 13, 1999 around noon.

Two special processing steps were applied on the map-projected AirMISR data. The first step was a first-order atmospheric correction. Based on Reagan sunphotometry, an aerosol optical depth of 0.135 in the green band was established, and a clean continental aerosol model consisting of 90% (by optical depth fraction) accumulation mode sulfate at 70% relative humidity, and 10% accumulation mode mineral dust was assumed and provided the atmospheric parameters needed to perform the surface retrieval. A surface pressure of 964.3 hPa was used to establish the Rayleigh scattering optical depth. Climatological atmospheric parameters such as ozone abundance were taken from the Terrestrial Atmosphere and Surface Climatology, or TASC dataset, which is an ancillary file set in conjunction with MISR standard data processing. Quantities needed for the radiative transfer calculation were derived from a lookup table generated to support MISR processing, known as the Simulated MISR Ancillary Radiative Transfer, or SMART, dataset [25].

The atmospheric correction was done on a camera-by-camera and band-by-band basis, and, for this purpose, the surface reflectance at angles not observed by the individual camera was assumed lambertian. This method does not distinguish between the hemispherical-directional reflectance factor and the bidirectional reflectance factor. The surface BRF was retrieved by first correcting for ozone absorption, subtracting off the path radiance, dividing by atmospheric direct and diffuse transmittance, and correcting for multiple reflections between the atmosphere and surface assuming reflectance homogeneity. The retrieved surface BRF was converted back to an equivalent radiance and the results were written out to AirMISR data files in the same format as the original data. The second processing step consisted of a pixel-by-pixel geometric remapping to improve the camera co-registration. The nadir image was used as a reference, and the Multipoint Matcher (M2) area matching algorithm developed for MISR stereo processing was used to determine the misregistration between each off-nadir camera and the nadir data [26]. Nine-by-nine pixel patches were used for the area matcher. For each pixel a cross-track and along-track misregistration, or disparity (in pixels) was determined. A smoothing algorithm consisting of a box filter was passed over the resulting disparity fields to eliminate blunders and fill in areas where the matching failed. The resulting disparity field was then used to "warp" the off-nadir imagery and a new data file consisting of the remapped data was written. For each camera, this processing was done band by band. Additional data fields containing the disparities were written to the data products for the off-nadir cameras.

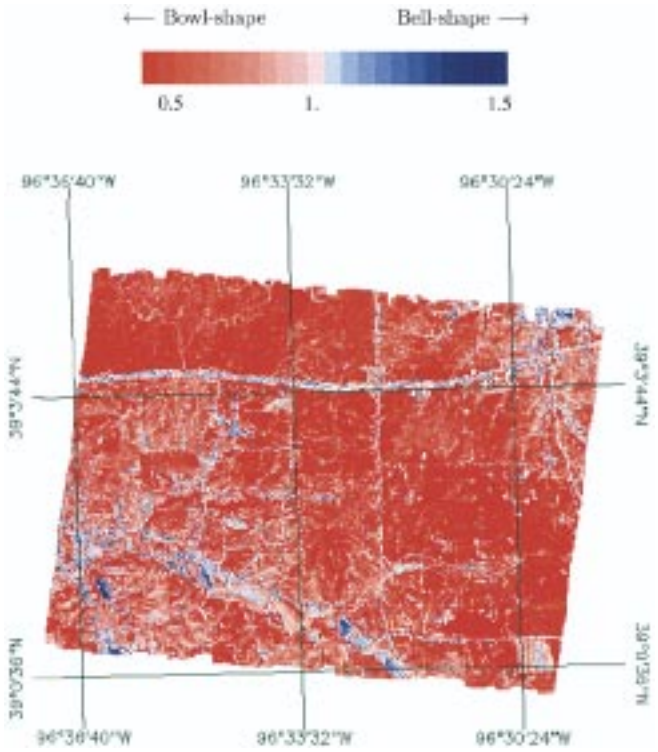

Fig. 6. Map of the parameter $k_{\rm red}$ obtained from an inversion of the RPV model against "surface BRF" data collected in the red band of the AirMISR instrument over Konza prairie on July 13, 1999. This BRF dataset was derived using a simplified atmospheric transfer scheme. The color code goes from red tones for low k values to blue tones for large k values and the intermediate white colors indicate pixels exhibiting values close to unity for the parameter k.

For the purpose of our investigation, the surface-level BRF dataset will be considered as if it were taken just above the surface without any corruption by atmospheric scattering effects. This dataset was further analyzed with the help of the RPV model in order to estimate, at the pixel resolution, the values of the parameter k.

Fig. 6 shows the map of the parameter $k_{\rm red}$ estimated in the red band, i.e., the spectral band which maximizes the single scattering effect as well as the required reflectance constrast between the soil and the vegetation. This map identifies a number of well-defined patterns which are directly related to the organization of the landscapes, i.e., some of the agricultural, pasture and other lands can be easily identified on the basis of the values depicted by the $k_{\rm red}$ parameter. As can be seen from the color convention adopted for the anisotropy shape parameter, some of these fields can be classified with respect to their bowl or bell-shape anisotropy pattern. A ground inspection of a number of these fields was conducted just about a year after the AirMISR data acquisition. It confirmed that the fields characterized by a bell-shaped anisotropy pattern exhibited some significant degree of heterogeneity at the scale of a few tens of meters. By contrast, a bowl-shape type of anisotropy was associated with those fields which do not exhibit strong vertical structures and 3-D heterogeneity at the scale of the AirMISR measurements. These features are qualitatively illustrated with the help of a series of photographs taken from the ground over a sample of the Konza fields (see Fig. 7 and further description in Table IV). A significant degree of heterogeneity, i.e., openings between vertically oriented and dense vegetation cover, was observed for nonmature maize fields as well as other more complex land surface types, indicating that the detected heterogeneous behavior orginates from very different types of land cover. Targets indentified as A and E provide good examples of the exposure of heterogeneity due to a strong contrast between the dense vertical vegetated structures and the bright soils which can be seen in the gaps between vegetation. An analogous situation occurs for the growing maize field, target B and C for instance; it can reasonably be anticipated that the heterogeneity will be progressively concealed (i.e., k values should decrease) as plants grow to close the canopy. By contrast, at the scale of the AirMISR pixels, the pasture fields (e.g., target F) which are not contaminated by significant vertical structures are characterized by a bowl-shaped anisotropy. Target D shows a case where the structural heterogeneity apparent from the photograph is not exposed by the analysis of the angular signature of the BRF field in the red domain, i.e., the value of k is close to 0.8; this result suggests that the coverage by green vegetation (instead of bright soil) of the horizontally wide gaps (with respect to the AirMISR spatial resolution) does not favor the detection of structural heterogeneity.

At this preliminary stage of investigation, the quantification of the degree of heterogeneity remains an open issue although the strategy recently proposed by [27] is promising. Nevertheless, the visual assessment of surface heterogeneity which can be made on the basis of this series of photographs confirms our expectations derived from simple reasoning and supported by extensive radiation transfer model simulations.

The dependency of the estimated values for the parameter k with respect to the resolution of the observing instrument can be examined on the basis of the AirMISR dataset. Indeed, in a first approximation, the local BRF values available from surface level BRF dataset can be iteratively aggregated in order to approximate BRF values that would have been measured by the same sensor but at different spatial resolutions. The upscaling process is achieved by calculating, from the original resolution of 27.5 m, the average values over windows of 2×2, 4×4, …, 32×32 pixels. This procedure thus permits relating the changes of the values of the parameter k against the sensor ground resolution. The series of panels in Fig. 8 display the results of such an upscaling approach when applied to the parameter $k_{\rm red}$. The progressive increase in the redish hue observed from the top left to bottom right panel confirms our expectation on the scale dependency, i.e., the lower the sensor resolution and the lesser its potential to expose the heterogeneous features invoking the 3-D organization of well-identified surface cover types. The spatial dimensions involved in this exercise, i.e., from $\approx$ 30 m up to 900 m, are indicative of the expected spatial scale and sensor resolution beyond which the angular signatures can hardly be used to detect a significantly heterogeneous situation even under favorable geophysical conditions.

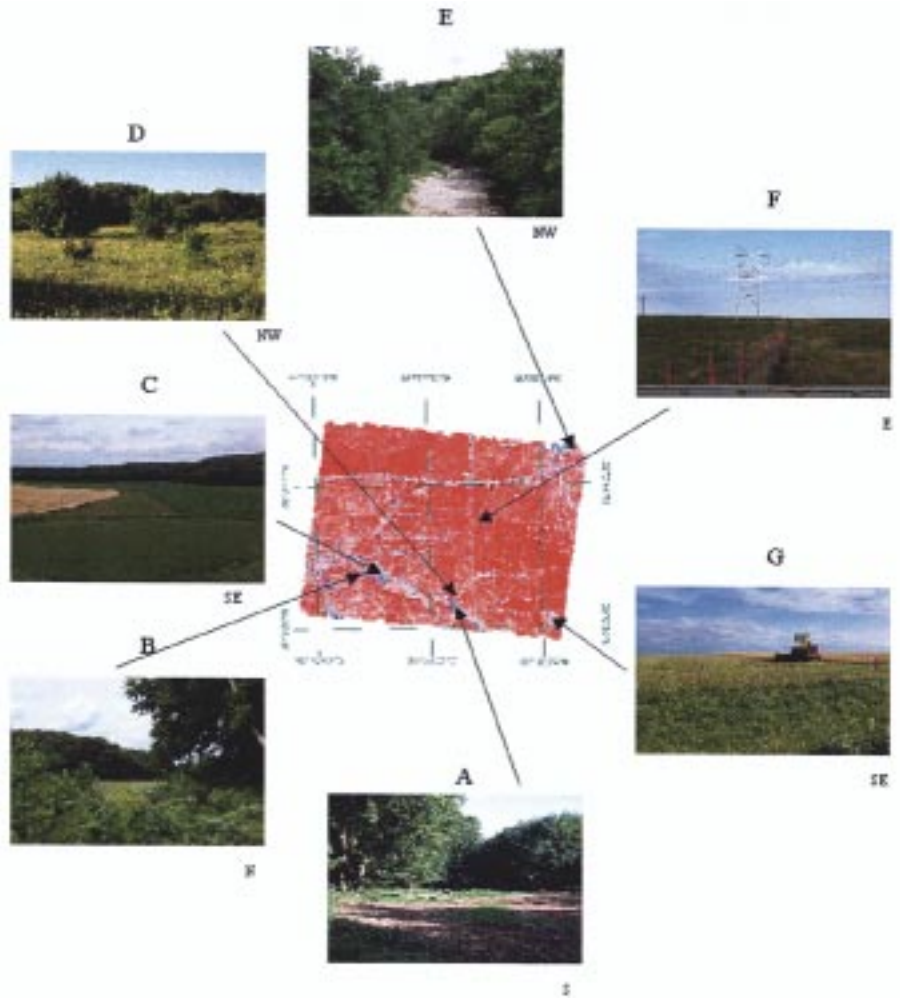

Fig. 7. Photographs illustrating the state of the landscapes over Konza prairie on June 7, 2000. The labeling permits co-locating the photographs with respect to the corresponding value of the parameter $k_{\rm red}$ mapped in Fig. 6. The approximate orientation of the views displayed are indicated below each photograph, i.e., N, S, E, and W stand for northward, southward, eastward, and westward directions, respectively.

V. Miscellaneous Issues

The concepts developed in this paper elicit further remarks on various related issues concerning both fundamental aspects of radiation transfer problems and immediate applications to the characterization of land surface properties, especially in the case of medium resolution sensors. The following issues arise in those regions detected as heterogeneous in the sense defined earlier:

- there is a discernable breakdown of the reciprocity principle due to the deviation from an homogeneous turbid plane-parallel system (see [28]). The application of models satisfying this basic principle must therefore be conducted with care, since, for instance, the use of these models against data acquired under various illumination conditions is not strictly valid. However, these models can be applied for the analysis of BRF fields sampled under a constant illumination angle. This conclusion is obviously not specific to the RPV model used here, but it holds for all models of this category;
- the spatio–temporal variations of the parameter k are partly controlled by the direction of illumination with respect to the target (see Fig. 5). Therefore, the value of this parameter cannot be interpreted directly as if it were an intrinsic surface property, e.g., the value of the parameter k may vary as a function of the season. However, a single instantaneous multiangular set of measurements may be sufficient to expose the heterogeneity of the region at the scale of investigation and to select further appropriate processing schemes;
- the acquisition of instantaneous BRF values by single angle view instruments, as available from most of the medium resolution scanning sensors, may fail in delivering accurate and reliable estimates of surface albedo when the algorithm emulates multiangular sampling from a sequential accumulation of BRF measurements over time. Indeed, during this time period of data accumulation, the values of the parameters entering the parametric models are not constant, which is contrary to the basic hypothesis supporting the approach;

TABLE IV
TARGET DESCRIPTIONS FROM THE SERIES OF PHOTOGRAPHS IN FIG. 7

Target	Description	Land category† from k values
A	Bare soil clearing, used by cattle, in a wooded area	**bell-shape**
B	Clearing used for maize cultivation in a wooded area	**bell-shape**
C	Transitions between senescent cereals (left), maize (middle) and full cover crop (right)	**bell-shape** for the maize field only
D	Natural meadow with shrubs	**bowl-shape**
E	Dry riverbed with shrubs	**bell-shape**
F	Two fields of permanent pasture separated by a fence	**bowl-shape** on both side of the fence
G	harvested and unharvested forage (background)	**bell-shape** for the harvested part only

† Bowl-shape (bell-shape) is assigned to pixels exhibiting k values belonging to the heterogeneity concealment (exposure) domain.

- the estimate of bihemispherical reflectance, which requires computing the integral of the directional hemispherical reflectance over all illumination angles [4], is not strictly valid if based on reciprocal models and thus assumes that the parameter values entering the model are not a function of the illumination angle (see, for instance, [15] and [29]);
- the extrapolation at other sun zenith angles of the directional hemispherical reflectance value estimated for one solar position may be unreliable following the argument given in the previous item;
- 3-D models should be used for inversion purposes whenever state variables are being retrieved from model inversions to the highest possible accuracy. In other words, 1-D radiation transfer models can be adopted in inversion procedures only over targets exhibiting a bowl-shaped anisotropy pattern, possibly using an IPA scheme to approximate solutions to the radiation transfer problem for mixed pixels. Depending on the sensor resolution, the choice of the appropriate model dimension to be applied can, however, hardly be made prior to the analysis of the data.

The interpretation of multiangular data acquired by medium and high spatial resolution sensors permits identifying those regions where a number of data analysis issues must be addressed. By contrast, approaches based on reciprocal models may be sufficient to analyze data for those regions where heterogeneity has not been detected. In other words, although all terrestrial surfaces present a degree of heterogeneity over a range of spatial scales, this fact does not imply *a priori* that the complexity of these surfaces has to be explicitly represented, since this complexity does not significantly influence the measured signal.

VI. CONCLUDING REMARKS

This paper stresses a unique capability offered by multiangular information for surface cover monitoring. Our approach is based on a straigthforward analysis of the BRF field sampled at red wavelengths, as available from data gathered by AirMISR and the MISR/Terra instruments. Our results strongly support the potential to map a class of surface cover heterogeneity from space data at the subpixel scale resolution, by simply setting a critical limit value for the parameter k_{red} estimated by the inversion of the RPV model; the occurrence of values larger than this limit indicates the very probable presence of a structurally heterogeneous surface. For typical vegetation systems, measurements in the red spectral region permit maximizing the required contrast between the scattering/absorption properties over the vegetation stands versus the underlying soil. Given the resolution of the observing in-

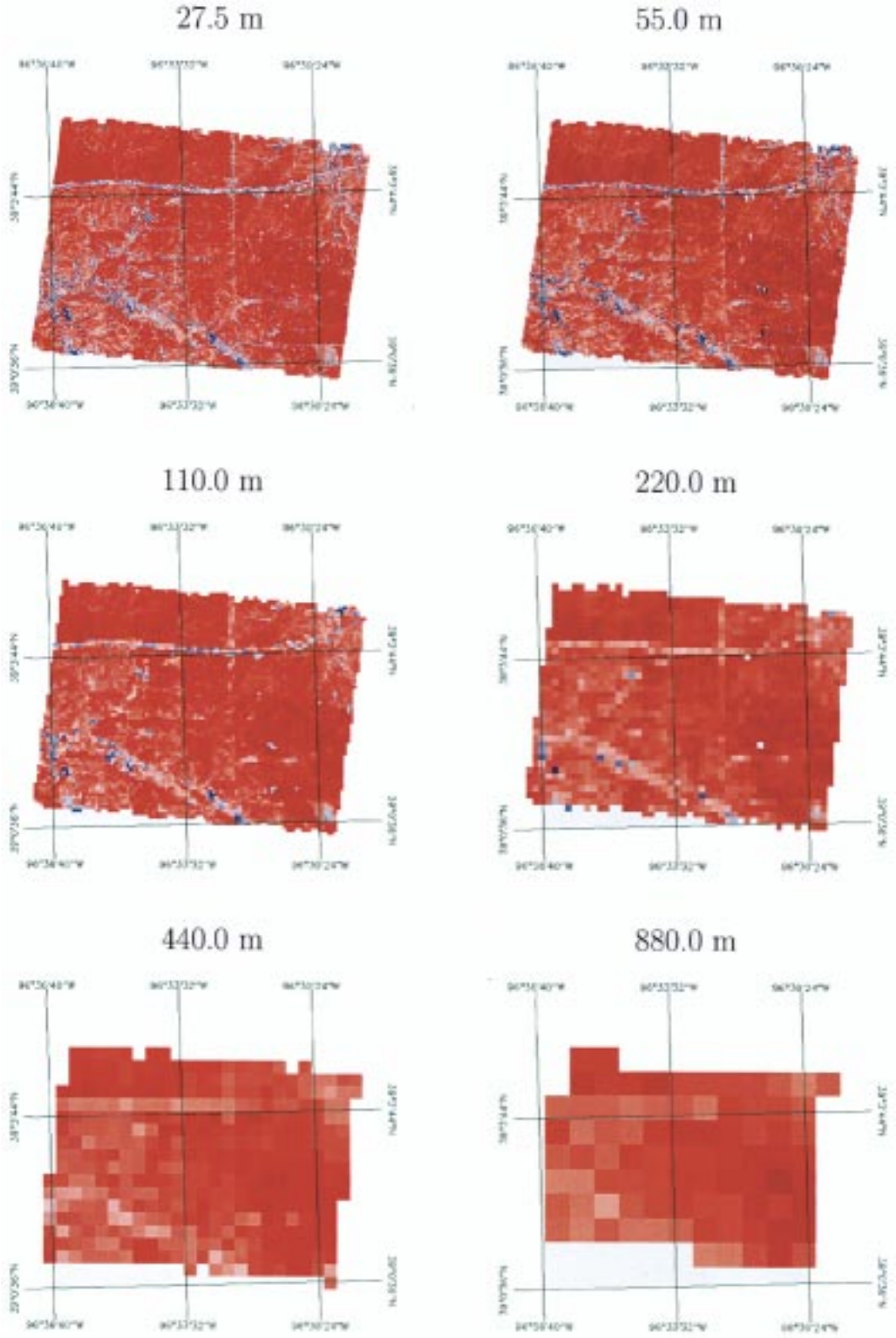

Fig. 8. Maps of the parameter k_{red} derived from an iterative aggregation the "surface BRF" data collected in the red band of the AirMISR instrument over Konza prairie on July 13, 1999. Conventions are the same as in Fig. 6. The simulated sensor resolution indicated on top of each panel decreases from the top left to the lower right panel.

strument, it was also shown that observation conditions made with near-overhead sun zenith angles favor the detectability of such heterogeneous vegetation. In practice, the processing involved to assess the value of the parameter k is straightforward, as the inversion of the RPV model can easily be made operational as discussed in the accompanying paper.

A series of applications, conducted with AirMISR and MISR data (see Part II), illustrate the potential benefit of exploiting the parameter k in land cover classification, since it reveals a different but complementary organization of the landscapes than can be already derived from instantaneous spectral information only. The sensor spatial resolution was shown to be of critical importance in the sense that the intrinsic landscape variability may result in a mixture between homogeneous and heterogenous surfaces. Thus, the decrease of the sensor spatial resolution renders the interpretation more complex, since it diminishes the relative weight of the information due to individual land cover with respect to each other and with respect to the topographical features as well. In other words, the typical dimensions involved in vegetation land cover type (e.g., height, size, and interdistance between trees) imposes a choice of sensor resolutions such that the BRF anisotropic shape can be further interpreted in terms of vegetation cover. No unique resolution thus permits documenting the vegetation heterogeneity for all surface types, but there is a range of resolutions that maximizes the probability of identifying the presence of architecturally organized plant stands. This issue stresses the need to establish the necessary links between the parameter k and a limited but critical set of descriptors of vegetation cover heterogeneity. As a first step, the approach described in [27] is very promising.

The exposure of subpixel scale surface heterogeneity from the analysis of an angular signature locates regions for which, at the scale of the investigation 1) the radiation transfer regime violates the reciprocity principle and 2) inversion procedures applied to retrieve vegetation properties to the highest possible accuracy, e.g., the leaf area index, should be based on 3-D radiation transfer models. This capability to detect significantly heterogeneous surfaces is important in the studies of long-term evolution of landscapes. Indeed, it has already been stressed that vegetation structure and its intrinsic dynamics can have a profound effect on ecosystem productivity, a key variable in understanding the vegetation response to climate change [30]. On the side of applications, it is noteworthy that this simple approach involving only one spectral band and the estimate of the parameter k should permit monitoring events such as the occurrence of snow on the ground as happens at the end of the Spring season in Boreal coniferous forests. Many other applications can be foreseen including those dealing with urban sprawl and crop monitoring, for instance.

Our analysis only involves the inversion of the RPV model and the further interpretation of the values of the parameter k. The arguments given in this paper are based on results from a conceptual model that were confirmed by extensive 3-D radiation transfer simulations. They provide the rationale for using the parameter k as a new axis of information in addition to the classical spectrally derived information. This issue is further addressed in the accompanying paper (Part II), which proposes a computer efficient method, optimized for the MISR instrument, to derive jointly information about the photosynthetic activity and the structure of the vegetation. It also addresses the practical issue of decontaminating the parameter k from atmospheric effects thereby allowing its fast estimation directly from data collected by the MISR instrument.

ACKNOWLEDGMENT

The motivation for this conceptual development demonstrating that a unique information can be extracted from multiangular data analysis came after an informal and stimulating discussion with W. Wiscombe. The application part presented here would not have been possible without the dedicated support from the scientific and technical team in charge of the AirMISR data acquisition and analysis. The authors thank the reviewers for very insightfull comments and recommendations on the first version of the manuscript.

REFERENCES

[1] D. J. Diner, G. P. Asner, R. Davies, Y. Knyazikhin, J.-P. Muller, A. W. Nolin, B. Pinty, C. B. Schaaf, and J. Stroeve, "New directions in earth observing: Scientific applications of multiangle remote sensing," *Bull. Amer. Meteorol. Soc.*, vol. 80, pp. 2209–2228, 1999.

[2] H. Rahman, B. Pinty, and M. M. Verstraete, "Coupled surface-atmosphere reflectance (CSAR) model. 2. Semiempirical surface model usable with NOAA advanced very high resolution radiometer data," *J. Geophys. Res.*, vol. 98, pp. 20 791–20 801, 1993.

[3] N. Gobron, B. Pinty, M. M. Verstraete, J.-L. Widlowski, and D. J. Diner, "Uniqueness of multi-angular measurements—Part II: Joint retrieval of vegetation structure and photosynthetic activity from MISR," *IEEE Trans. Geosci. Remote Sensing*, vol. 40, pp. 1574–1592, July 2002.

[4] J. V. Martonchik, C. J. Bruegge, and A. H. Strahler, "A review of reflectance nomenclature for remote sensing," *Remote Sens. Rev.*, vol. IWMMM-2, 2000.

[5] B. Pinty and M. M. Verstraete, "Modeling the scattering of light by vegetation in optical remote sensing," *J. Atmos. Sci.*, vol. 55, pp. 137–150, 1998.

[6] N. Gobron, B. Pinty, M. M. Verstraete, J. V. Martonchik, Y. Knyazikhin, and D. J. Diner, "The potential of multi-angular spectral measurements to characterize land surfaces: Conceptual approach and exploratory application," *J. Geophys. Res.*, vol. 105, pp. 17 539–17 550, 2000.

[7] M. M. Verstraete, B. Pinty, and R. B. Myneni, "Potential and limitations of information extraction on the terrestrial biosphere from satellite remote sensing," *Remote Sens. Environ.*, vol. 58, pp. 201–214, 1996.

[8] W. Lucht and J.-L. Roujean, "Considerations in the parametric modeling of BRDF and albedo from multiangular satellite sensor observations," *Remote Sens. Rev.*, vol. 18, pp. 343–379, 2000.

[9] W. Wanner, X. Li, and A. H. Strahler, "On the derivation of kernels for kernel-driven models of bidirectional reflectance," *J. Geophys. Res.*, vol. 100, pp. 21 077–21 089, 1995.

[10] O. Engelsen, B. Pinty, M. M. Verstraete, and J. V. Martonchik, "Parametric bidirectional reflectance factor models: Evaluation, improvements and applications," EC Joint Research Centre, Ispra, Italy, EUR 16 426 EN, 1996.

[11] M. Minnaert, "The reciprocity principle in lunar photometry," *Astrophys. J.*, vol. 93, pp. 403–410, 1941.

[12] L. G. Henyey and T. L. Greenstein, "Diffuse radiation in the galaxy," *Astrophys. J.*, vol. 93, pp. 70–83, 1941.

[13] B. Pinty, F. Roveda, M. M. Verstraete, N. Gobron, Y. Govaerts, J. Martonchik, D. Diner, and R. Kahn, "Surface albedo retrieval from METEOSAT—Part 2: Application," *J. Geophys. Res.*, vol. 105, pp. 18 113–18 134, 2000.

[14] H. Jacobowitz, H. V. Soule, H. L. Kyle, and F. B. House, "The earth radiation budget (ERB) experiment: An overview," *J. Geophys. Res.*, vol. 89, pp. 5021–5038, 1984.

[15] J. V. Martonchik, D. J. Diner, B. Pinty, M. M. Verstraete, R. B. Myneni, Y. Knyazikhin, and H. R. Gordon, "Determination of land and ocean reflective, radiative, and biophysical properties using multiangle imaging," *IEEE Trans. Geosci. Remote Sensing*, vol. 36, pp. 1266–1281, 1998.

[16] W. Ni and D. Jupp, "Spatial variance in directional remote sensing imagery—Recent developments and future perspectives," *Remote Sensing Rev.*, vol. 18, pp. 441–479, 2000.

[17] F. F. Gerard and P. R. J. North, "Analyzing the effect of structural variability and canopy gaps on forest BRDF using a geometric-optical model," *Remote Sens. Environ.*, vol. 62, pp. 46–62, 1997.

[18] Y. Govaerts and M. M. Verstraete, "Raytran: A monte carlo ray tracing model to compute light scattering in three-dimensional heterogeneous media," *IEEE Trans. Geosci. Remote Sensing*, vol. 36, pp. 493–505, 1998.

[19] N. Gobron, B. Pinty, M. M. Verstraete, and Y. Govaerts, "A semi-discrete model for the scattering of light by vegetation," *J. Geophys. Res.*, vol. 102, pp. 9431–9446, 1997.
[20] R. F. Cahalan, W. Ridgway, W. J. Wiscombe, T. L. Bell, and J. B. Snider, "The albedo of fractal stratocumulus clouds," *J. Atmos. Sci.*, vol. 51, pp. 2434–2455, 1994.
[21] B. Pinty, N. Gobron, J.-L. Widlowski, S. A. W. Gerstl, M. M. Verstraete, M. Antunes, C. Bacour, F. Gascon, J.-P. Gastellu, N. Goel, S. Jacquemoud, P. North, W. Qin, and R. Thompson, "The radiation transfer model intercomparison (RAMI) exercise," *J. Geophys. Res.*, vol. 106, pp. 11 937–11 956, 2001.
[22] N. Gobron and D. Lajas, "A new inversion scheme for the RPV model," Can. J. Remote Sensing, 2002, to be published.
[23] J. C. Price, "Examples of high resolution visible to near-infrared reflectance spectra and a standardized collection for remote sensing studies," *Int. J. Remote Sensing*, vol. 16, pp. 993–1000, 1995.
[24] D. J. Diner, L. M. Barge, C. J. Bruegge, T. G. Chrien, J. E. Conel, M. L. Eastwood, J. D. Garcia, M. A. Hernandez, C. G. Kurzweil, W. C. Ledeboer, N. D. Pignatano, C. M. Sarture, and B. G. Smith, "The airborne multi-angle imaging spectroradiometer AirMISR instrument description and first results," *IEEE Trans. Geosci. Remote Sensing*, vol. 36, pp. 1339–1349, 1998.
[25] D. J. Diner, W. A. Abdou, H. R. Gordon, R. A. Kahn, Y. Knyazikhin, J. V. Martonchik, S. McMuldroch, R. B. Myneni, and R. A. West, "MISR Level 2 Ancillary Products and Datasets Algorithm Theoretical Basis," NASA Jet Propulsion Lab., Pasadena, CA, JPL D-13 402, 1997.
[26] D. J. Diner, R. Davies, L. D. Girolamo, A. Horvath, C. Moroney, J.-P. Muller, S. R. Paradise, D. Wenkert, and J. Zong, "MISR Level 2 Cloud Detection and Classification Algorithm Theoretical Basis," NASA Jet Propulsion Lab., Pasadena, CA, JPL D-11 399, 1997.
[27] J.-L. Widlowski, B. Pinty, N. Gobron, M. M. Verstraete, and A. B. Davies, "Characterization of surface heterogeneity detected at the MISR/TERRA subpixel scale," *Geophys. Res. Lett.*, vol. 28, pp. 4639–4642, 2001.
[28] S. Chandrasekhar, *Radiative Transfer*. New York: Dover, 1960.
[29] W. Lucht, "Expected retrieval accuracies of bidirectional reflectance and albedo from EOS-MODIS and MISR angular sampling," *J. Geophys. Res.*, vol. 103, pp. 8763–8778, 1998.
[30] H. H. Shugart, "Importance of structure in the longer-term dynamics of landscapes," *J. Geophys. Res.*, vol. 105, pp. 20 065–20 075, 2000.

Bernard Pinty received the Maitrise de Chimie and DEA degrees in 1977, the these de troisieme cycle en Physique de l'Atmosphere degree in 1980, and the these d'Etat degree in 1988, all from the Université Blaise Pascal, Clermont-Ferrand, France.

He visited the National Center for Atmospheric Research (NCAR), Boulder, CO, in 1988–1989, served as Deputy Director of the Laboratoire d'Etudes et de Recherches en Teledetection Spatiale (LERTS), Toulouse, France, in 1990–1992, and was appointed Full Professor of physics at the Universite Blaise Pascal in 1993. He is currently with the Institute for Environment and Sustainability (IES), Ispra, Italy. He received the Zel'dovich medal from COSPAR (1990) and is a member of the MERIS Scientific Advisory Group of the European Space Agency, and a member of the MISR Science Team of NASA/JPL. His main interests currently include research on the theory of radiation transfer in plant canopies, and, more generally, the development of tools to quantitatively interpret satellite remote sensing data in the optical spectral domain.

Jean-Luc Widlowski received the B.Sc. degree in geophysics and planetary physics from the University of Newcastle upon Tyne, U.K., in 1993, the M.Sc. degree in remote sensing and image processing technology from the University of Edinburgh, U.K., in 1995, and the Ph.D. degree from the University of Fribourg, Switzerland, in 2002.

He is currently with the Institute for Environment and Sustainability (IES), Ispra, Italy, developing advanced methods for the extraction of quantitative information on terrestrial surface heterogeneity at the subpixel scale.

Nadine Gobron (M'01) received the Maitrise de Physique degree in 1993, the DEA in Sciences de la Terre et de l'Atmosphere degree in 1994, and the doctorat d'universite en Physique de l'Atmosphere in 1997 from the Universite Blaise Pascal, Clermont-Ferrand, France.

She had a Post Doctoral fellowship from ESA in 1998 and JRC in 1999, and was, until 2001, a Staff Member of the Institute for Environment and Sustainability (IES), Ispra, Italy. She has developed physically-based algorithms to retrieve land surface products for instruments of ESA (MERIS/ENVISAT), NASA (SeaWiFS/OrbView-2 and MISR/TERRA), NASDA (GLI), and CNES (VEGTATION). She is an Associate Member of the MISR Science Team. Her main interests currently include the modeling of radiation transfer and the design of advanced methods to extract quantitative information from remote sensing data in the solar domain.

Michel M. Verstraete (M'95) received the License en Physique in 1974 from the Universite Catholique de Louvain, Louvain-la-Neuve, Belgium, the License Speciale en Geophysique in 1976 from the Universite Libre de Bruxelles, Belgium, and the M.Sc. degree in meteorology in 1978 as well as the D.Sc. degree in atmospheric sciences in 1985 from the Massachusetts Institute of Technology, Cambridge.

He worked for the World Meteorological Organization (WMO), Geneva, Switzerland and Nairobi, Kenya, from 1979 to 1981, at the National Center for Atmospheric Research (NCAR), Boulder, CO), from 1982 to 1989, taught at the University of Michigan, Ann Arbor, in 1989–1990, and is currently with the Institute for Environment and Sustainability (IES), Ispra, Italy. He is a member of various scientific advisory committees (e.g., MERIS) of the European Space Agency (ESA) and co-investigator of the MISR Science Team of NASA/JPL. His initial work on topics such as the modeling of atmosphere-biosphere interactions and desertification lead him to his current interest in the quantitative exploitation of satellite remote sensing data for the characterization of terrestrial surface properties.

David J. Diner (A'01) received the B.S. degree in physics (with honors) from the State University of New York at Stony Brook in 1973 and the M.S. and Ph.D. degrees in planetary science from the California Institute of Technology, Pasadena, in 1977 and 1978, respectively.

He has been with the Jet Propulsion Laboratory, Pasadena, since 1981. He is currently a Principal Member of the Technical Staff and Leader of the Multi-angle Imaging Science Element in the Earth and Space Sciences Division. He has been involved in numerous NASA planetary and Earth remote-sensing investigations, and is Principal Investigator of the MISR experiment and its airborne counterpart, AirMISR.

Dr. Diner is a member of the American Geophysical Union and the IEEE Geoscience and Remote Sensing Society.